GEOPHYSICS, VOL. 66, NO. 3 (MAY-JUNE 2001); P. 897–903, 4 FIGS., 1 TABLE.

Depth-domain velocity analysis in VTI media using surface *P*-wave data: Is it feasible?

Yves Le Stunff*, Vladimir Grechka‡, and Ilya Tsvankin‡

ABSTRACT

The main difficulties in anisotropic velocity analysis and inversion using surface seismic data are associated with the multiparameter nature of the problem and inherent trade-offs between the model parameters. For the most common anisotropic model, transverse isotropy with a vertical symmetry axis (VTI media), *P*-wave kinematic signatures are controlled by the vertical velocity V_0 and the anisotropic parameters ϵ and δ. However, only two combinations of these parameters—NMO velocity from a horizontal reflector $V_{\mathrm{nmo}}(0)$ and the anellipticity coefficient η—can be determined from *P*-wave reflection traveltimes if the medium above the reflector is laterally homogeneous. While $V_{\mathrm{nmo}}(0)$ and η are sufficient for time-domain imaging in VTI media, they cannot be used to resolve the vertical velocity and build velocity models needed for depth migration.

Here, we demonstrate that *P*-wave reflection data can be inverted for all three relevant VTI parameters (V_0, ϵ and δ) if the model contains nonhorizontal intermediate interfaces. Using anisotropic reflection tomography, we carry out parameter estimation for a two-layer medium with a curved intermediate interface and reconstruct the correct anisotropic depth model. To explain the success of this inversion procedure, we present an analytic study of reflection traveltimes for this model and show that the information about the vertical velocity and reflector depth was contained in the reflected rays which crossed the dipping intermediate interface.

The results of this work are especially encouraging because the need for depth imaging (such as prestack depth migration) arises mostly in laterally heterogeneous media. Still, we restricted this study to a relatively simple model and constrained the inversion by assuming that one of the layers is isotropic. In general, although lateral heterogeneity does create a dependence of *P*-wave reflection traveltimes on the vertical velocity, there is no guarantee that for more complicated models all anisotropic parameters can be resolved in a unique fashion.

INTRODUCTION

This paper discusses the influence of lateral heterogeneity (in the form of dipping interfaces along the raypath) on the results of parameter estimation for transversely isotropic media with a vertical axis of symmetry (VTI). To constrain the anisotropic velocity model using surface data, it is beneficial to record reflected rays spanning a wide range of propagation directions (e.g., Alkhalifah and Tsvankin, 1995; Tsvankin and Thomsen, 1995). Angle coverage of reflection data can be increased by processing dipping events or long-offset data from horizontal interfaces. Wide-angle recording, however, implies that the rays cover a relatively large subsurface area and may be influenced by lateral heterogeneity in the form of either smooth velocity variations or dip and irregular shape of intermediate interfaces. In general, lateral heterogeneity may significantly complicate the inversion process by introducing additional trade-offs between the model parameters. (Note that the problem of separating the contribution of lateral velocity variation to reflection traveltimes from that of the shape of interfaces is known to be quite involved even for isotropic media; see Goldin, 1986.) It turns out, however, that as long as the subsurface structure and the velocity model remain relatively simple, lateral heterogeneity can actually help in constraining the parameters which are impossible to obtain in similar models with a homogeneous or horizontally layered overburden. This point is illustrated here for a two-layer VTI medium with a dipping intermediate interface.

Manuscript received by the Editor May 24, 1999; revised manuscript received April 17, 2000.
*Formerly Totalfina Exploration and Production, Route de Versailles, 78470 St. Remy les Chevreuse, France; presently Total Austral, Calle Moreno 877-Piso 19, 1091 Buenos Aires, Argentina. E-mail: Yves.Le-Stunff@total.com.
‡Colorado School of Mines, Center for Wave Phenomena, Dept. of Geophysics, Golden, Colorado 80401-1887. E-mail: vgrechka@ dix.mines.edu; ilya@dix.mines.edu.

Parameter estimation in transversely isotropic media has attracted considerable attention in the literature in the past several years (e.g., Bube and Meadows, 1997; Bartel et al., 1998; Grechka and Tsvankin, 1998; Le Stunff and Grenié, 1998; Le Stunff and Jeannot, 1998; Sexton and Williamson, 1998). One of the common conclusions that can be drawn from these publications is that surface P-wave reflection data in VTI media are inherently insufficient to constrain the vertical velocity and reflector depth. Analytic support for this result is provided by the work of Alkhalifah and Tsvankin (1995), who showed that P-wave reflection traveltimes are fully controlled by only two parameters—the NMO velocity from a horizontal reflector $V_{\rm nmo}(0)$ and the anellipticity coefficient η:

$$V_{\rm nmo}(0) = V_0\sqrt{1+2\delta}, \tag{1}$$

$$\eta \equiv \frac{\epsilon-\delta}{1+2\delta}. \tag{2}$$

Here, V_0 is the P-wave vertical velocity, and ϵ and δ are Thomsen's (1986) anisotropy parameters; V_0, ϵ, and δ fully control P-wave kinematic signatures in VTI media (Tsvankin, 1996). Since the vertical velocity contributes to $V_{\rm nmo}(0)$ [equation (1)] only in combination with δ, it seems that P-wave traveltime data cannot be used to resolve V_0 and determine the depth scale in VTI media. Therefore, one has to rely on additional information (e.g., borehole data or shear waves) in building anisotropic velocity models for prestack and poststack depth migration.

The Alkhalifah-Tsvankin (1995) result, however, was derived for *laterally homogeneous* VTI media above a dipping reflector. The presence of lateral heterogeneity in the subsurface may, in principle, cause dependence of P-wave reflection traveltimes on the individual values of V_0, ϵ, and δ. Such a dependence was indeed observed by Alkhalifah et al. (1998), who commented, however, that the dependence was rather weak for the models they tested. Grechka and Tsvankin (1999) developed a general methodology for obtaining NMO velocities in laterally heterogeneous media and used it to demonstrate that P-wave NMO velocities from reflectors beneath layered VTI media with *nonhorizontal* intermediate interfaces may contain information about the layers' thicknesses. They emphasized that the dip of intermediate interfaces makes the P-wave reflection data dependent on all three Thomsen parameters (V_0, ϵ, and δ). Hence, an important practical issue is whether for a certain class of laterally heterogeneous VTI models the parameters V_0, ϵ, and δ can be determined unambiguously from surface P-wave data.

Without attempting to answer this question in full generality, we present a successful synthetic example of P-wave reflection tomography in a layered VTI model with a curved intermediate interface. Our results prove that P-wave reflection traveltimes in some piecewise homogeneous VTI models can indeed be inverted for the parameters V_0, ϵ, and δ, along with the depths and dips of the reflecting interfaces. We begin with a description of our numerical test and then give an analytic explanation of the results using the theory of Grechka and Tsvankin (1999).

TOMOGRAPHIC INVERSION FOR A TWO-LAYER MODEL

The model chosen for tomographic parameter estimation is shown in Figure 1. It contains two homogeneous layers (VTI and isotropic) separated by a curved interface. The traveltimes of P-waves reflected from both interfaces were calculated by ray tracing; the acquisition parameters are listed in Table 1.

We added Gaussian noise with zero mean and a standard deviation of 2.5 ms to the traveltimes to simulate picking errors and applied a tomographic algorithm (e.g., Stork and Clayton, 1985; Kaculini and Guiziou, 1992) to perform traveltime inversion. The initial model was purely isotropic with the parameters estimated from conventional time-to-depth conversion using the NMO velocities and zero-offset traveltimes. The tomographic procedure updates the model to minimize the misfit between the input and computed traveltimes using a linearized least-squares algorithm (Tarantola, 1987). We constrained the inversion assuming that

1) the model consists of two homogeneous layers,
2) the bottom layer is isotropic, and
3) the bottom reflector is horizontal.

The intermediate interface was parameterized by a B-spline with 12 nodes (one node per every 40 common midpoints). The model parameters include the vertical velocity $V_{\rm t}$ (t stands for "top") and the coefficients $\epsilon_{\rm t}$ and $\delta_{\rm t}$ in the VTI layer, the velocity $V_{\rm b}$ (b stands for "bottom") in the isotropic layer, the depth $Z_{\rm r}$ of the horizontal reflector, and the spline coefficients responsible for the shape and position of the intermediate interface. At each iteration all parameters were updated simultaneously. As shown in Figure 2, the algorithm successfully converges toward the correct solution after only a few iterations. Note that since we determined both velocities $V_{\rm t}$ and $V_{\rm b}$, we can reconstruct the actual depths and dips of both interfaces. Clearly, in this example P-wave reflection traveltimes provide enough information for building a model in the *depth* domain.

The results of our tomographic experiment may seem to contradict the theory of Alkhalifah and Tsvankin (1995), as well as the conclusions of some recent publications cited above. For

Table 1. Acquisition parameters used in ray tracing. The number of receivers per CMP gather and the maximum offset were reduced for CMP locations near the edges of the model.

Parameter	Value
Number of common midpoints	500
CMP spacing	12.5 m
Number of receivers per CMP gather	40
Receiver spacing	100 m
Minimum offset	0 m
Maximum offset	4000 m

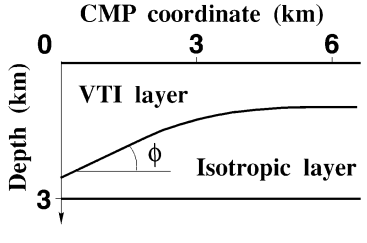

FIG. 1. The model used for tomographic parameter estimation. The top layer is VTI with the P-wave vertical velocity $V_{\rm t} = 2.5$ km/s and the anisotropic coefficients $\epsilon_{\rm t} = 0.2$ and $\delta_{\rm t} = 0.05$. The bottom layer is isotropic with the P-wave velocity $V_{\rm b} = 3.5$ km/s; the depth of the lower boundary $Z_{\rm r} = 3$ km. The intermediate interface has the dip $\phi = 25^\circ$ at the zero CMP coordinate and is horizontal on the right.

instance, Bube and Meadows (1997) state that in TI media "… the well-known velocity-depth ambiguity cannot be separated as it can be done in the isotropic case." Indeed, velocity–depth ambiguity in our model cannot be overcome using the reflection from the intermediate interface that yields only the parameters $V_{\mathrm{nmo,t}}(0)$ and η_{t} in the VTI layer [see equations (1) and (2)] (Alkhalifah and Tsvankin, 1995). Including the reflection from the bottom interface near the right edge of the model where both interfaces are horizontal (Figure 1), one can also determine the velocity V_{b} in the isotropic layer from the conventional Dix (1955) equation. The quantities $V_{\mathrm{nmo,t}}(0)$ and η_{t}, however, provide sufficient information only for time processing and do not constrain the thickness of the VTI layer.

Below, we show that the success of the tomographic inversion procedure was ensured by the traveltimes from the bottom reflector near the left edge of the model, where the intermediate interface is *dipping*. This dip causes the dependence of P-wave moveout on all four relevant parameters (V_{t}, V_{b}, ϵ_{t}, and δ_{t}), thus constraining the depth scale of the model.

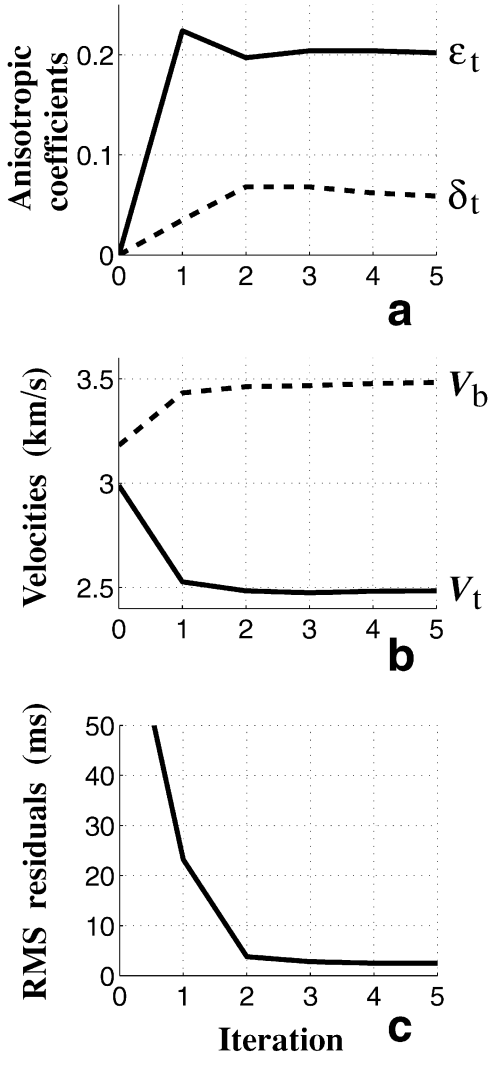

FIG. 2. The model parameters and time residuals obtained by the iterative inversion algorithm. (a) Anisotropic coefficients ϵ_{t} and δ_{t}; (b) velocities V_{t} and V_{b}; and (c) rms traveltime residuals. The residuals at the fourth and fifth iterations are equal to the standard deviation of the noise (2.5 ms) added to the data.

ANALYTIC EXPLANATION OF THE INVERSION RESULTS

Slopes of the zero-offset reflections

In the dip-moveout (DMO) inversion algorithm of Alkhalifah and Tsvankin (1995), the slopes of reflection events are supposed to be determined from the zero-offset time section and used as the arguments of the NMO-velocity function. As mentioned above, the DMO inversion in the VTI layer yields the values of the zero-dip NMO velocity $V_{\mathrm{nmo,t}}(0)$ and η_{t} but not the true vertical velocity. The dip of the intermediate interface, however, also creates a dependence of the slope of the bottom reflection (p_{b}) on the parameters of the top (VTI) layer.

As shown in Appendix A, the value of p combined with the slope p_{t} of the reflection from the intermediate dipping interface (Figure 3a) can be used to infer the vertical velocity V_{t}. Under the assumption of weak anisotropy and mild dip of the intermediate interface, the relation between the two slopes is given by [equation (A-6)]

$$p_{\mathrm{b}} V_{\mathrm{b}} \approx p_{\mathrm{t}}(V_{\mathrm{b}} - V_{\mathrm{t}}). \tag{3}$$

Since the velocity V_{b} in the isotropic layer can be obtained using the Dix differentiation near the right edge of the model (see above), equation (3) yields the velocity V_{t}. For our model, calculating V_{t} directly from equation (3) yields $V_{\mathrm{t}} = 2.42$ km/s, which is reasonably close to the correct value $V_{\mathrm{t}} = 2.5$ km/s. Then, since the zero-dip NMO velocity $V_{\mathrm{nmo,t}}(0)$ can be determined from moveout analysis on the right-hand side of the model, we can use equation (1) to obtain the anisotropic coefficient δ_{t}. Note that if the intermediate interface is horizontal, $p_{\mathrm{b}} = p_{\mathrm{t}} = 0$ and equation (3) contains no information about the velocities.

NMO velocity from the bottom reflector

Although, as discussed above, the zero-offset reflection slopes are already sufficient for resolving the vertical velocity in the VTI layer using reflection tomography for the whole model, here we show that additional information about V_{t} is provided by the NMO velocity of the bottom reflection event on the left-hand side of the model. As before, we assume that the zero-dip NMO velocity $V_{\mathrm{nmo,t}}(0)$ and η_{t} were determined using the data from the right-hand side of the model and the NMO velocity $V_{\mathrm{nmo,t}}(p_{\mathrm{t}})$ from the intermediate interface (dashed line in Figure 3b). Then, as follows from the work of Grechka and Tsvankin (1999), the NMO velocity $V_{\mathrm{nmo,b}}(p_{\mathrm{b}})$ from the bottom horizontal reflector on the left-hand side of the model (solid line in Figure 3b) can be inverted for the coefficient δ_{t} and the vertical velocity V_{t} in the VTI layer. Two results of Grechka and Tsvankin (1999) applicable to our problem can be briefly summarized as follows.

1) Normal-moveout velocity of any pure-mode reflection plotted from the common midpoint along all possible directions of CMP lines in 3-D space forms a quadratic NMO-velocity surface, which usually is either a one-sheeted hyperboloid, or a cylinder, or an ellipsoid. If the medium at the common midpoint is locally homogeneous, the surface has to be a cylinder with the axis parallel to the zero-offset ray at the CMP location.

2) Dix-type averaging and differentiation procedures in piecewise homogeneous media are applicable to the cross-sections of the NMO-velocity cylinders by intermediate interfaces.

Here, we discuss a 2-D version of Grechka-Tsvankin's (1999) Dix-type averaging procedure that is adequate for our test model (Figure 1). Since both layers are homogeneous and the model is two-dimensional, the NMO-velocity surfaces of all reflections are cylinders with the axes confined to the vertical incidence plane. Cross-sections of these cylinders by the interfaces will represent ellipses (or circles in special cases) with the axes in the incidence plane and orthogonal to it. Since in our tomographic experiment we did not measure traveltimes outside the incidence plane, we apply the averaging scheme of Grechka and Tsvankin just to the in-plane axes of the cross-sections.

Figure 4 illustrates the process of building the effective NMO velocity $V_{\mathrm{nmo,b}}$ for the reflection from the bottom interface on the left-hand side of our model (the intermediate interface is assumed to be planar). $V_{\mathrm{cyl,b}}$ and $V_{\mathrm{cyl,t}}$ are the semiaxes (gray lines in Figures 4a and 4b; full axes are shown) of the cross-sections of two interval NMO-velocity cylinders (dashed lines in Figures 4a and 4b) by the intermediate interface. Following Grechka and Tsvankin (1999), these axes have to be averaged according to the Dix (1955) formula,

$$V^2_{\mathrm{cyl,eff}} = \frac{\tau_{\mathrm{b}} V^2_{\mathrm{cyl,b}} + \tau_{\mathrm{t}} V^2_{\mathrm{cyl,t}}}{\tau_{\mathrm{b}} + \tau_{\mathrm{t}}}, \qquad (4)$$

where τ_{b} and τ_{t} are the zero-offset traveltimes in the bottom and top layers (Figures 4a and 4b). $V_{\mathrm{cyl,eff}}$ is the effective NMO velocity in the direction parallel to the intermediate interface (gray line in Figure 4c). Finally, the NMO velocity $V_{\mathrm{nmo,b}}(p_{\mathrm{b}})$ (Figure 4d) on a surface CMP line is found by projecting $V_{\mathrm{cyl,eff}}$ along the axes of the NMO-velocity cylinder (dashed lines in Figure 4d) onto the horizontal plane.

The result of this averaging operation can be written as (Appendix B)

$$V^2_{\mathrm{nmo,b}}(p_{\mathrm{b}}) = \frac{V^2_{\mathrm{b}}(1 - q'_{\mathrm{b}} \tan\phi)^2}{1 + \tau_{\mathrm{t}}/\tau_{\mathrm{b}}} + \frac{V^2_{\mathrm{nmo,t}}(p_{\mathrm{b}})}{1 + \tau_{\mathrm{b}}/\tau_{\mathrm{t}}}, \qquad (5)$$

where p_{b}, as above, is the slope of the reflection from the horizontal interface on the zero-offset section (i.e., the horizontal component of the slowness vector of the zero-offset ray taken at the surface), $q'_{\mathrm{b}} \equiv dq_{\mathrm{b}}/dp_{\mathrm{b}}$ is the derivative of the vertical slowness component q_{b} at the surface with respect to p_{b}, and

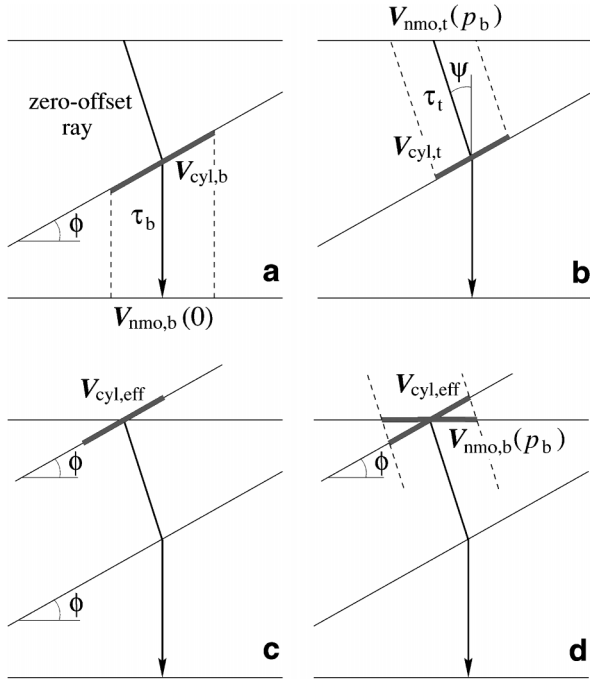

FIG. 4. Two-dimensional version of the Dix-type averaging procedure (Grechka and Tsvankin, 1999) for a two-layer model with an intermediate dipping interface. $V_{\mathrm{cyl,b}}$ (a) and $V_{\mathrm{cyl,t}}$ (b) are the in-plane semiaxes (full axes are shown) of the cross-sections of the interval NMO-velocity cylinders in the isotropic (bottom) and VTI layers. Dix-type averaging of $V_{\mathrm{cyl,b}}$ and $V_{\mathrm{cyl,t}}$ produces the in-plane axis $V_{\mathrm{cyl,eff}}$ (c) of the cross-section of the effective NMO-velocity cylinder. $V_{\mathrm{cyl,eff}}$ is then projected along the effective cylinder onto the horizontal plane, yielding the NMO velocity $V_{\mathrm{nmo,b}}(p_{\mathrm{b}})$ (d) measured at the surface.

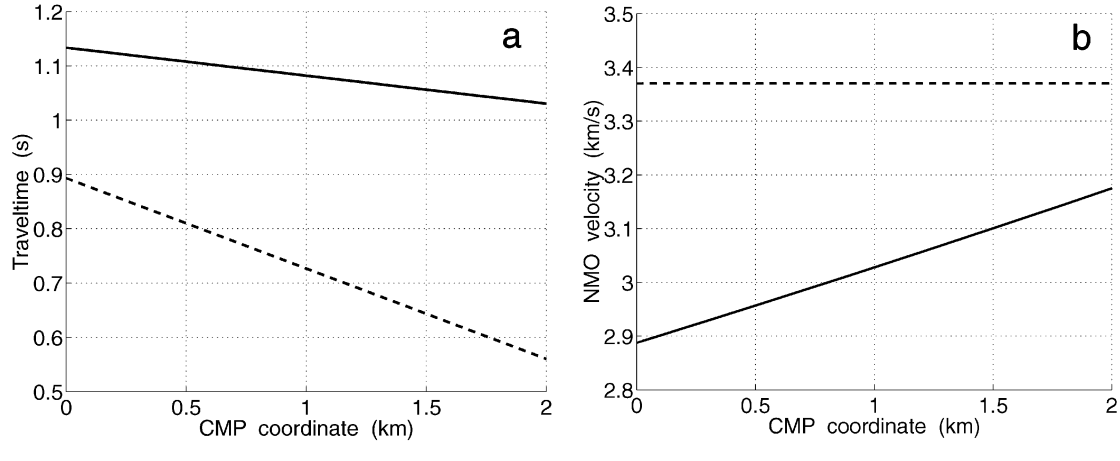

FIG. 3. Zero-offset traveltimes and NMO velocities on the left-hand side of the model (Figure 1) where the dip of the intermediate interface is constant. (a) One-way zero-offset traveltimes of the events reflected from the bottom horizontal interface (solid line) and intermediate dipping interface (dashed). The slopes of these events (p_b and p_{t}, respectively) can be used to constrain the vertical velocity V_{t} in the top (VTI) layer. (b) NMO velocities from the bottom interface [$V_{\mathrm{nmo,b}}(p_b)$; solid line] and the intermediate interface [$V_{\mathrm{nmo,t}}(p_{\mathrm{t}})$; dashed line].

$V_{\mathrm{nmo,t}}(p_\mathrm{b})$ (Figure 4b) is the NMO velocity from the bottom of the VTI layer corresponding to the same value of p_b [i.e., $V_{\mathrm{nmo,t}}(p_\mathrm{b})$ corresponds to the horizontal cross-section of the interval NMO-velocity cylinder in the VTI layer].

Next, we analyze equation (5) to show that the NMO velocity $V_{\mathrm{nmo,b}}(p_\mathrm{b})$ depends on δ_t for given values of $V_{\mathrm{nmo,t}}(0)$ and η_t. Note that the normal-moveout velocity $V_{\mathrm{nmo,t}}(p_\mathrm{b})$ in the numerator of the second term is a function of just p_b, η_t, and $V_{\mathrm{nmo,t}}(0)$ with no separate dependence on δ_t (Alkhalifah and Tsvankin, 1995). In contrast, δ_t does contribute to the numerator of the first term through the product $q' \tan\phi$. The simplest way to demonstrate that $q'_\mathrm{b} \tan\phi$ is indeed a function of δ_t is to obtain its approximation in the weak-anisotropy limit [equation (B-8) in Appendix B]:

$$q'_\mathrm{b} \tan\phi \approx V_\mathrm{b} \left[p_\mathrm{b} V_{\mathrm{nmo,t}}(0)\right]^2 \frac{V_{\mathrm{nmo,t}}(0)(1+\delta_\mathrm{t}) - V_\mathrm{b}}{\left[V_{\mathrm{nmo,t}}(0) - V_\mathrm{b}\right]^2}. \quad (6)$$

It can be shown that δ_t also influences the ratio of the traveltimes in the two layers ($\tau_\mathrm{t}/\tau_\mathrm{b}$). This ratio, unlike the term $q'_\mathrm{b} \tan\phi$, changes with the CMP coordinate X_CMP, which makes $V_{\mathrm{nmo,b}}(p_\mathrm{b})$ from equation (5) a laterally varying function as well (Figure 3b). From the structure of equation (5) and the fact that $q'_\mathrm{b} \tan\phi$ is not a function of X_CMP, it is clear that the dependence of $q'_\mathrm{b} \tan\phi$ on δ_t cannot be compensated by the traveltime ratio $\tau_\mathrm{t}/\tau_\mathrm{b}$ for all CMP locations.

We conclude that the NMO velocity of the bottom event $V_{\mathrm{nmo,b}}(p_\mathrm{b})$ as a whole depends on the anisotropic parameter δ_t in addition to $V_{\mathrm{nmo,t}}(0)$ and η_t. According to equation (5), our ability to invert $V_{\mathrm{nmo,b}}(p_\mathrm{b})$ for the parameter δ_t and, consequently, for the depth of the intermediate interface is tied to the interface dip ϕ. The greater the dip, the better δ_t and the vertical velocity V_t are constrained by the reflection traveltimes. If the intermediate interface is horizontal, $V_{\mathrm{nmo,b}}(p_\mathrm{b}=0)$ is completely independent of δ_t because $q'_\mathrm{b} \tan\phi = 0$.

Inversion on the left-hand side of the model

Our analytic results show that the presence of the dipping intermediate interface plays a crucial role in constraining the vertical velocity V_t in the VTI layer. In the discussion above, however, we assumed that the velocities $V_{\mathrm{nmo,t}}(0)$ and V_b were obtained from moveout analysis on the right-hand side of the model (Figure 1). Below, we demonstrate that this assumption is in fact unnecessary, and it is possible to find all VTI parameters using *only* the traveltimes near the left edge of the model.

Neglecting the curvature of the intermediate interface, the left-hand side of the model can be fully described by the following seven parameters: the dip ϕ and the depth Z_i (e.g., at the zero CMP coordinate $X_\mathrm{CMP}=0$) of the intermediate interface; the depth Z_r of the horizontal reflector; the parameters V_t, ϵ_t, and δ_t which control P-wave kinematics in the VTI layer; and the velocity V_b in the bottom isotropic layer. As indicated by Figure 3, surface data may contain enough information to resolve all these parameters. The zero-offset traveltimes in Figure 3a are linear functions of the CMP coordinate X_CMP and therefore provide a total of four constraints (i.e., four equations for the unknown parameters). The NMO velocity $V_{\mathrm{nmo,t}}(p_\mathrm{t})$ from the dipping interface (Figure 3b) does not depend on X_CMP, thus adding one more equation. Two more equations come from the NMO velocity $V_{\mathrm{nmo,b}}(p_\mathrm{b})$ of the bottom event (Figure 3b) that depends almost linearly on X_CMP.

Thus, the traveltime data on the left-hand side of the model yield seven nonlinear equations for seven unknown parameters. We have solved these equations by the simplex method and have obtained accurate estimates of the model parameters close to those determined from reflection tomography (Figure 2).

DISCUSSION AND CONCLUSIONS

Lateral heterogeneity is commonly perceived as one of the main hindrances in velocity analysis and parameter estimation, especially if the medium is anisotropic. Therefore, it is not surprising that parameter estimation in VTI media has been largely based on the theory by Alkhalifah and Tsvankin (1995) developed for *laterally homogeneous* overburden above a horizontal or dipping reflector. The results of Alkhalifah and Tsvankin (1995) clearly show that P-wave reflection traveltimes and time imaging in such a model are fully controlled by the vertical traveltime and just two parameters—the zero-dip NMO velocity $V_\mathrm{nmo}(0)$ and the anisotropic coefficient η. While the extension of time-domain velocity analysis and imaging to VTI media produced a number of impressive results (such as superior imaging of dipping reflectors), the problem of building anisotropic models for depth imaging without using additional information (e.g., borehole data or *PS*-waves) remained unresolved.

This work demonstrates that for certain types of *laterally heterogeneous* VTI media it may be feasible to invert P-wave moveout for all three relevant Thomsen parameters (the vertical velocity V_0 and the anisotropic coefficients ϵ and δ) and therby to find the depth-dependent velocity field. Our model included a VTI layer with a curved lower boundary overlying a purely isotropic layer. Analytic expressions for the reflection slopes and NMO velocities show that the information about the vertical velocity and thickness of the VTI layer was contained in the reflection event transmitted through the *dipping* intermediate interface.

Although we succeeded in using reflection tomography for depth-domain parameter estimation in a two-layer VTI model and corroborated the obtained results theoretically, the unique solution may no longer exist if the model is more complicated. For instance, if the bottom layer becomes anisotropic (VTI), the traveltimes on the left-hand side of the model are no longer sufficient for recovering the vertical velocities. Indeed, the number of available equations remains the same (seven), but the number of unknowns increases as a result of the addition of the anisotropic coefficients in the bottom layer. Evidently, while the dip of intermediate interfaces and possibly some other relatively simple types of lateral heterogeneity may be helpful in anisotropic velocity analysis, the range of laterally heterogeneous VTI models susceptible to the unambiguous tomographic inversion of reflection traveltimes should be rather restricted. A systematic analysis of P-wave moveout inversion for layered VTI media with planar and irregular interfaces will be given in our sequel publications.

ACKNOWLEDGMENTS

We are grateful to P. Williamson (Elf) for his review of the manuscript. Y. Le Stunff thanks J. P. Jeannot and P. Hardy (GX Technology) for their contribution to the tomography software. V. Grechka and I. Tsvankin were partially supported by

the members of the Consortium Project on Seismic Inverse Methods for Complex Structures at the Center for Wave Phenomena, Colorado School of Mines, and by the United States Department of Energy (award DE-FG03-98ER14908). I. Tsvankin also acknowledges the Shell Foundation for providing a Shell Faculty Career Initiation Grant.

REFERENCES

Alkhalifah, T., and Tsvankin, I., 1995, Velocity analysis in transversely isotropic media: Geophysics, **60**, 1550–1566.
Alkhalifah, T., Biondi, B., and Fomel, S., 1998, Time-domain processing in arbitrary inhomogeneous media: 68th Ann. Internat. Mtg., Soc. Expl. Geophys., Expanded Abstracts, 1756–1759.
Bartel, D. C., Abriel, W. L., Meadows, M. A., and Hill, N. R., 1998, Determination of transversely isotropic velocity parameters at the Pluto Discovery, Gulf of Mexico: 68th Ann. Internat. Mtg., Soc. Expl. Geophys., Expanded Abstracts, 1269–1272.
Bube, K. P., and Meadows, M. A., 1997, On the null space in linearized anisotropic surface reflection tomography: 67th Ann. Internat. Mtg., Soc. Expl. Geophys., Expanded Abstracts, 1677–1680.
Dix, C. H., 1955, Seismic velocities from surface measurements: Geophysics, **20**, 68–86.
Goldin, S. V., 1986, Seismic traveltime inversion: Soc. Expl. Geophys.
Grechka, V., and Tsvankin, I., 1998, 3-D description of normal moveout in anisotropic inhomogeneous media: Geophysics, **63**, 1079–1092.
———1999, NMO surfaces and Dix-type formulae in heterogeneous anisotropic media: 69th Ann. Internat. Mtg., Soc. Expl. Geophys., Expanded Abstracts, 1612–1615.
Grechka, V., Tsvankin, I., and Cohen, J. K., 1999, Generalized Dix equation and analytic treatment of normal-moveout velocity for anisotropic media: Geophys. Prosp., **47**, 117–148.
Kaculini, S., and Guiziou, J. L., 1992, Prestack reflection tomography in practice: 62nd Ann. Internat. Mtg., Soc. Expl. Geophys., Expanded Abstracts, 1046–1049.
Le Stunff, Y., and Grenié, D., 1998, Taking into account a priori information in 3D tomography: 68th Ann. Internat. Mtg., Soc. Expl. Geophys., Expanded Abstracts, 1875–1878.
Le Stunff, Y., and Jeannot, J. P., 1998, Pre-stack anisotropic depth imaging: 60th EAGE Conference, Extended Abstracts.
Sexton, P., and Williamson, P., 1998, 3-D anisotropic velocity estimation by model-based inversion of pre-stack traveltimes: 68th Ann. Internat. Mtg., Soc. Expl. Geophys., Expanded Abstracts, 1855–1858.
Stork, C., and Clayton, R. W., 1985, Iterative tomographic and migration reconstruction of seismic images: 55th Ann. Internat. Mtg., Soc. Expl. Geophys., Expanded Abstracts, 610–613.
Tarantola, A., 1987, Inverse problem theory: Methods for data fitting and model parameter estimation: Elsevier Science Publ. Co., Inc.
Thomsen, L., 1986, Weak elastic anisotropy: Geophysics, **51**, 1954–1966.
Tsvankin, I., 1996, *P*-wave signatures and notation for transversely isotropic media: An overview: Geophysics, **61**, 467–483.
Tsvankin, I., and Thomsen, L., 1995, Inversion of reflection traveltimes for transverse isotropy: Geophysics, **60**, 1095–1107.

APPENDIX A

SLOPES OF THE REFLECTION EVENTS IN THE TOMOGRAPHIC MODEL

Here we find an approximate relation between the slopes of the zero-offset reflections from the bottom and intermediate interfaces in the model from Figure 1. To simplify the derivation, we assume that the anisotropy in the VTI layer is weak and the dip of the interface is mild.

The zero-offset ray reflected from the bottom of the model is vertical (i.e., perpendicular to the reflector) in the isotropic layer and becomes oblique in the top (VTI) layer. The horizontal slowness component of this ray at the surface (denoted as p_b) determines the slope of the bottom reflection on the zero-offset time section. Applying Snell's law at the intermediate interface yields an expression that involves p_b and the interface dip ϕ:

$$p_b + \tan\phi\left[\frac{1}{V_b} - q_b\right] = 0, \tag{A-1}$$

where V_b is the velocity in the bottom layer and q_b is the vertical slowness component of the zero-offset ray at the surface.

Using the weak-anisotropy version of the Christoffel equation, we obtain the following expression for q_b linearized in the anisotropic parameters δ_t and η_t:

$$q_b = \frac{(1+\delta_t)(1-y) - \eta_t y^2}{V_{nmo,t}(0)\sqrt{1-y}}, \tag{A-2}$$

where $V_{nmo,t}(0)$ is the zero-dip NMO velocity in the VTI layer and $y \equiv [p_b V_{nmo,t}(0)]^2$. Substituting equation (A-2) into equation (A-1) and linearizing the result in the anisotropic coefficients yields

$$\begin{aligned}\tan\phi &= p_b\left[\frac{1+\delta_t}{V_{nmo,t}(0)} - \frac{1}{V_b}\right]^{-1} + O\left(p_b^3\right)\\ &= p_b\left[\frac{1}{V_t} - \frac{1}{V_b}\right]^{-1} + O\left(p_b^3\right),\end{aligned} \tag{A-3}$$

where V_t is the vertical P-wave velocity in the top VTI layer. Cubic and higher powers of p_b in equation (A-3) are not shown explicitly because the corresponding terms should be small for mild dips.

The dip ϕ can also be found using the reflection from the intermediate interface. Since the slowness vector $[p_t, q_t]$ of the zero-offset reflected ray is orthogonal to the interface,

$$\tan\phi = \frac{p_t}{q_t}. \tag{A-4}$$

Combining equation (A-2) (where q_b should be replaced by q_t and p_b by p_t) and equation (A-4) allows us to express $\tan\phi$ through the slope p_t:

$$\tan\phi = p_t V_t + O\left(p_t^3\right). \tag{A-5}$$

Substituting equation (A-3) into (A-5) and retaining only linear terms in p_t and p_b leads to the following relation between the slopes of the two reflection events:

$$p_b = p_t\left(1 - \frac{V_t}{V_b}\right). \tag{A-6}$$

APPENDIX B

NMO VELOCITY FROM THE BOTTOM REFLECTOR

The P-wave NMO velocity $V_{\mathrm{nmo,b}}$ for the bottom reflection event (Figure 4) can be found using the general formalism developed by Grechka and Tsvankin (1999). As discussed in the main text, the Dix-type expressions of Grechka and Tsvankin operate with the (elliptical) cross-sections of NMO-velocity cylinders by the model interfaces. In our 2-D problem, we will need to obtain only the in-plane axes of these cross-sections (i.e., the axes confined to the vertical incidence plane).

First, we have to find the velocities $V_{\mathrm{cyl,b}}$ and $V_{\mathrm{cyl,t}}$ (gray lines in Figures 4a and 4b), which correspond to the cross-sections of the interval NMO cylinders by the intermediate interface. The NMO-velocity cylinder in the bottom layer (dashed lines in Figure 4a) is circular with the axis parallel to the vertical segment of the zero-offset ray. The radius of the circle at the bottom of the NMO-velocity cylinder is simply equal to the velocity V_{b} because the bottom layer is isotropic. As illustrated by Figure 4a, the cross-section $V_{\mathrm{cyl,b}}$ of the cylinder by the intermediate interface is given by

$$V_{\mathrm{cyl,b}} = \frac{V_{\mathrm{b}}}{\cos\phi}. \tag{B-1}$$

Equation (B-1) is the familiar expression for the dip-component of NMO velocity in isotropic media.

The axis of the NMO-velocity cylinder in the VTI layer is parallel to the group velocity vector (i.e., to the zero-offset ray; see Figure 4b). The angle ψ between the zero-offset ray and vertical can be written as (Grechka et al., 1999)

$$\tan\psi = -\frac{dq_{\mathrm{b}}}{dp_{\mathrm{b}}} \equiv -q_{\mathrm{b}}', \tag{B-2}$$

where p_{b} and q_{b} are the horizontal and vertical slowness components of the zero-offset ray in the VTI layer. The quantity $V_{\mathrm{nmo,t}}(p_{\mathrm{b}})$ in Figure 4b corresponds to the dip component of the NMO velocity from a dipping reflector (nonexistent in our model) orthogonal to the slowness vector $\{p_{\mathrm{b}}, q_{\mathrm{b}}\}$. $V_{\mathrm{nmo,t}}(p_{\mathrm{b}})$ has to be projected onto the intermediate dipping interface along the axes of the NMO-velocity cylinder (dashed lines in Figure 4b). This projection, denoted by $V_{\mathrm{cyl,t}}$, can be determined from the law of sines:

$$V_{\mathrm{cyl,t}} = V_{\mathrm{nmo,t}}(p_{\mathrm{b}})\frac{\cos\psi}{\cos(\psi-\phi)}. \tag{B-3}$$

Substituting $\tan\psi$ from equation (B-2) yields

$$V_{\mathrm{cyl,t}} = \frac{V_{\mathrm{nmo,t}}(p_{\mathrm{b}})}{\cos\phi(1-q_{\mathrm{b}}'\tan\phi)}. \tag{B-4}$$

The second step in our derivation is the Dix averaging of the velocities $V_{\mathrm{cyl,b}}$ and $V_{\mathrm{cyl,t}}$ described by equations (B-1) and (B-4):

$$V^2_{\mathrm{cyl,eff}} = \frac{1}{\tau_{\mathrm{b}}+\tau_{\mathrm{t}}}\left[\tau_{\mathrm{b}}\frac{V_{\mathrm{b}}^2}{\cos^2\phi} + \tau_{\mathrm{t}}\frac{V^2_{\mathrm{nmo,t}}(p_{\mathrm{b}})}{\cos^2\phi(1-q_{\mathrm{b}}'\tan\phi)^2}\right], \tag{B-5}$$

where τ_{b} and τ_{t} are the zero-offset traveltimes in the bottom and top layers. The averaged velocity $V_{\mathrm{cyl,eff}}$ corresponds to the cross-section of the effective NMO-velocity cylinder by a plane parallel to the dipping interface (gray line in Figure 4c).

Finally, we project $V_{\mathrm{cyl,eff}}$ onto the horizontal plane to obtain the NMO velocity $V_{\mathrm{nmo,b}}(p_{\mathrm{b}})$ (Figure 4d) of the bottom reflection event that can be measured from surface data. This projection can be found directly from equations (B-3) and (B-4):

$$\begin{aligned} V_{\mathrm{nmo,b}}(p_{\mathrm{b}}) &= V_{\mathrm{cyl,eff}}\frac{\cos(\psi-\phi)}{\cos\psi} \\ &= V_{\mathrm{cyl,eff}}\cos\phi(1-q_{\mathrm{b}}'\tan\phi). \end{aligned} \tag{B-6}$$

Substituting equation (B-5) into equation (B-6) leads to the final result:

$$V^2_{\mathrm{nmo,b}}(p_{\mathrm{b}}) = \frac{\tau_{\mathrm{b}}V_{\mathrm{b}}^2(1-q_{\mathrm{b}}'\tan\phi)^2 + \tau_{\mathrm{t}}V^2_{\mathrm{nmo,t}}(p_{\mathrm{b}})}{\tau_{\mathrm{b}}+\tau_{\mathrm{t}}}. \tag{B-7}$$

Equation (B-7) is almost identical to the conventional Dix (1955) formula, but it contains the factor $(1-q_{\mathrm{b}}'\tan\phi)^2$ that appears because of the dip ϕ of the intermediate interface. To gain insight into the dependence of $q_{\mathrm{b}}'\tan\phi$ on the model parameters, we simplify this expression, assuming that the dip ϕ is small (i.e., $|\tan\phi| \ll 1$) and anisotropy is weak (i.e., $|\delta_{\mathrm{t}}| \ll 1$ and $|\eta_{\mathrm{t}}| \ll 1$). The derivative q_{b}' can be obtained by differentiating equation (A-2), while $\tan\phi$ is given by equation (A-3). Keeping only linear terms in the anisotropic coefficients and terms up to quadratic in the slope p_{b}, we find

$$\begin{aligned} q_{\mathrm{b}}'\tan\phi = {} & V_{\mathrm{b}}[p_{\mathrm{b}}V_{\mathrm{nmo,t}}(0)]^2\frac{V_{\mathrm{nmo,t}}(0)(1+\delta_{\mathrm{t}})-V_{\mathrm{b}}}{[V_{\mathrm{nmo,t}}(0)-V_{\mathrm{b}}]^2} \\ & + O\left(p_{\mathrm{b}}^4\right). \end{aligned} \tag{B-8}$$

Clearly, even for weak anisotropy the term $q_{\mathrm{b}}'\tan\phi$ depends not only on the NMO velocity $V_{\mathrm{nmo,t}}(0)$ but also on the anisotropic coefficient δ_{t}; implications of this result are discussed in the main text.